A Large-Scale Analysis on Contextual Self-Supervised Video Representation Learning

Akash Kumar[1†]   Ashlesha Kumar[2]   Vibhav Vineet[3]   Yogesh Singh Rawat[1]

CRCV, University of Central Florida[1]   BITS Pilani[2]   Microsoft Research[3]

Abstract

Self-supervised learning has emerged as a powerful paradigm for label-free model pretraining, particularly in the video domain, where manual annotation is costly and time-intensive. However, existing self-supervised approaches employ diverse experimental setups, making direct comparisons challenging due to the absence of a standardized benchmark. In this work, we establish a unified benchmark that enables fair comparisons across different methods. Additionally, we systematically investigate five critical aspects of self-supervised learning in videos: (1) dataset size, (2) model complexity, (3) data distribution, (4) data noise, and (5) feature representations. To facilitate this study, we evaluate six self-supervised learning methods across six network architectures, conducting extensive experiments on five benchmark datasets and assessing performance on two distinct downstream tasks. Our analysis reveals key insights into the interplay between pretraining strategies, dataset characteristics, pretext tasks, and model architectures. Furthermore, we extend these findings to Video Foundation Models (ViFMs), demonstrating their relevance in large-scale video representation learning. Finally, leveraging these insights, we propose a novel approach that significantly reduces training data requirements while surpassing state-of-the-art methods that rely on 10× more pretraining data. We believe this work will guide future research toward a deeper understanding of self-supervised video representation learning and its broader implications.

1. Introduction

Deep learning models require a large amount of labeled data for their training. Obtaining annotations at large-scale needs a lot of effort and it becomes even more challenging as we shift from image to video domain. There are several interesting directions focusing on this issue such as domain adaptation [84], knowledge distillation [22], semi-supervised learning [87], self-supervision [33] and weakly-supervised learning [65], which attempts to rely on the knowledge learned from existing source datasets and transfer to new target datasets with minimal labels. Among these approaches, self-supervised learning use pretext task as supervisory signal and does not require any labels on source datasets which makes it more favorable.

In recent years, self-supervised learning (SSL) has made significant progress in video representation learning [10, 34, 56, 78, 85, 88]. More recently, research has shifted towards context-based learning, which involves modifying input data to derive a classification [13, 34, 83, 85], reconstruction [10, 88], or generative [26, 53, 68, 73, 77] signal that serves as a learning objective. The primary focus of these approaches is to design pretext tasks that are computationally efficient while providing a strong supervisory signal, enabling models to learn meaningful *spatio-temporal* features.

Despite these advancements, comparing different SSL methods remains challenging due to the absence of standardized evaluation protocols. Existing approaches are assessed under varying conditions, lacking a common benchmark to ensure fair and consistent evaluation. A recent study [72] takes a step in this direction by analyzing downstream learning; however, it does not explore the self-supervision aspect, which is the primary focus of our work.

In this study, we introduce a benchmark where key self-supervised pretraining parameters are standardized across methods to enable fair comparisons. Using this benchmark, we systematically investigate five critical aspects of self-supervised learning: (1) the effect of pretraining dataset size, (2) task complexity, (3) generalization under distribution shifts, (4) robustness against data noise, and (5) properties of the learned representations. Fig. 1 provides an overview.

Our benchmark conducts a large-scale evaluation of representative context-based self-supervised methods for video representation learning. We analyze two key factors: (1) the *learning objective*, differentiating between *contrastive* and *non-contrastive* methods, and (2) *data transformations*, categorized into *spatial*, *temporal*, and *spatio-temporal* variations. We examine six pretext tasks across six different architectures, conducting experiments on five action recognition

---

[1†]Corresponding Author: akash.kumar@ucf.edu
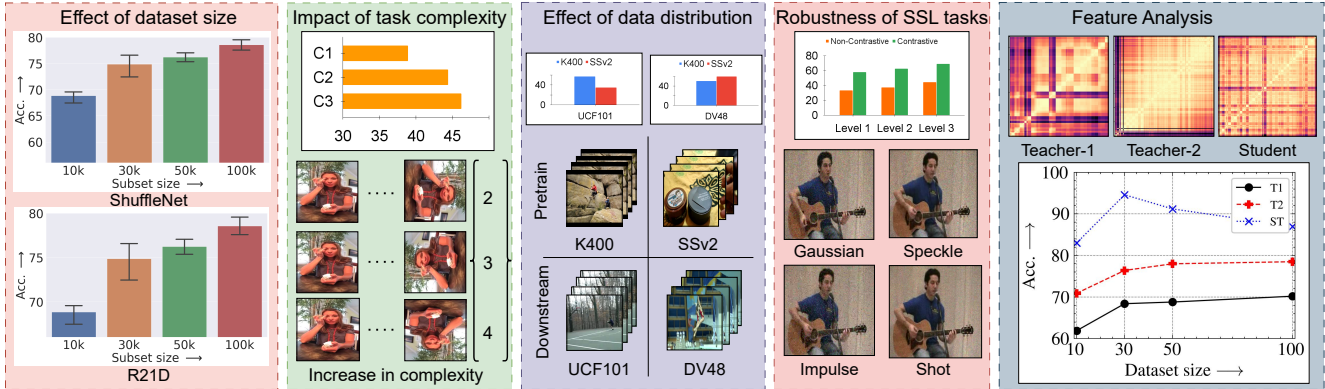
Figure 1. **Overview of proposed benchmark.** We study five different aspects in this benchmark study. Starting from left, 1) we show the analysis of *effect of dataset size vs training time*. As the dataset size increases, variation in performance decreases even with longer training time, 2) We show the effect of *task complexity* (C1, C2, C3 - Different complexities). Bottom figure shows use case of how complexity increases for the RotNet task, and, top figure shows how the performance varies for the R21D network, 3) With different *data distribution shifts*, the third sub-figure shows the impact of *target* data distribution on the *source* data, 4) We look into another data distribution shift due to introduction of noise. We see how *non-contrastive* tasks are more robust than *contrastive* ones even with increasing levels of severity of noise. The bottom part shows an example for each type of noise. Clips are provided in supplementary, and, 5) Finally, we further analyze whether the features learn *orthogonal* information. In this sub-figure, we show that using different architectures as teachers can substantially improve performance even in a low-data regime.

datasets and evaluating these approaches on two downstream tasks: action recognition and video retrieval. Furthermore, we extend our study to recently developed video foundation models.

Our findings reveal several key insights: (1) contrastive learning methods converge faster but exhibit lower robustness to data noise, (2) increasing pretext task complexity does not necessarily lead to better spatio-temporal representation learning, (3) *temporal* pretext tasks are more challenging than *spatial* or *spatio-temporal* ones, (4) spatio-temporal tasks demonstrate robustness to distribution shifts, and (5) pretext tasks learn complementary features across different architectures, dataset distributions, dataset sizes, and pretext task types.

Our contributions are threefold:

- We introduce a benchmark for self-supervised video representation learning, ensuring fair comparisons of different pretext tasks under a unified experimental setup.
- We conduct an extensive analysis of five critical factors in self-supervised learning for videos: (1) dataset size, (2) task complexity, (3) distribution shifts, (4) data noise, and (5) feature representations.
- Finally, we validate our insights by proposing a simple yet effective approach that surpasses existing state-of-the-art methods on video action recognition while requiring significantly less pretraining data. Additionally, we provide a structured recipe for future self-supervised learning methods to build upon.

We believe our study will serve as a foundation for advancing self-supervised video representation learning and guiding future research in the field.

2. Related Work

Self-supervised learning   Several studies have explored self-supervised learning (SSL) for video representation learning [33, 64] for efficient labeling amongst other approaches such as semi-supervised [14, 41, 44, 50, 57, 58, 66] and weakly-supervised [21, 43].   These approaches can be broadly categorized based on the nature of the pretext task: (1) context-based methods [3, 10, 13, 17, 20, 25, 32, 36, 56, 59, 71, 78, 81, 83, 86] and (2) cross-modal methods [1, 55, 62].   Cross-modal approaches leverage multiple modalities, such as audio, video, optical flow, and camera viewpoints, relying on cross-modal consistency to learn representations. In contrast, context-based learning utilizes transformations within a single modality to generate supervisory signals. Over the years, context-based pretraining tasks have evolved significantly, focusing on understanding how different transformations impact learned representations. Unlike cross-modal approaches, context-based methods explicitly exploit spatial and temporal information through various transformations [7, 20, 49, 56, 78, 83, 85]. Recent works have extended these methods by jointly transforming both spatial and temporal domains [10, 36, 48, 71, 88]. While incorporating multiple modalities can enhance performance, such data is often unavailable for large-scale datasets. Therefore, in this work, we focus exclusively on single-modality (RGB) approaches.

Self-supervised benchmarking   Several prior studies have focused on benchmarking SSL in the image domain. In [23], the authors provide an in-depth analysis of self-supervised image representation learning, investigating how dataset

scaling influences learned representations. Similarly, [37] examines the role of different model architectures in self-supervised learning. However, both studies primarily focus on downstream performance rather than analyzing the pretext tasks themselves. Their primary objective is to improve specific pretext tasks rather than to study their underlying impact on representation learning. In contrast, we systematically analyze various pretext tasks and evaluate how different factors influence feature learning. Additionally, while previous studies primarily focus on the image domain, our work extends this analysis to videos. [19] explores unsupervised learning in the video domain by adapting pretext tasks from images to videos. However, their primary emphasis remains on downstream evaluation. Our work differs by focusing on the self-supervised aspect itself, analyzing key factors such as dataset size, task complexity, data distribution, and robustness to noise. By addressing these aspects, we provide a comprehensive understanding of how different pretraining strategies affect video representation learning. A recent study [42] looks into similar aspect but hasn't looked into video foundation models which corresponds to the ftre ahead.

3. Self-Supervised Configurations

We first describe the pretext tasks used in our study along with their categorization followed by details of this benchmark including network architectures, datasets, downstream tasks and evaluations.

3.1. Task Categorization

We analyze video pretext tasks from two key perspectives: (1) the transformations applied to the data and (2) the learning objectives. The data transformations fall into three categories: *spatial-based (S)*, *temporal-based (T)*, and *spatio-temporal (ST)*. *Spatial* transformations involve reshuffling spatial patches, applying temporally consistent data augmentations, or rotating images and patches. *Temporal* tasks focus on frame/clip permutation classification, order verification, clip sampling at different playback rates, or contrastive learning using temporal triplets. *Spatio-temporal* tasks simultaneously modify both spatial and temporal dimensions. Examples include dilated sampling with frame reconstruction, joint spatial and temporal shuffling, speed prediction, and contrastive learning of visual features.

The learning objectives can be categorized as either *contrastive* [11] or *non-contrastive* [88]. Based on this categorization, we select at least two representative pretext tasks from each transformation category, ensuring inclusion of both contrastive and non-contrastive methods. Specifically, we study the following pretext tasks: RotNet (Rot) [34], Video Clip Order Prediction (VCOP) [85], Playback Rate Prediction (PRP) [88], Spatiotemporal Contrastive Video Representation Learning (CVRL) [56], Temporal Discriminative Learning (TDL) [78], and Relative Speed Perception

Network (RSPNet) [10]. A detailed description of these tasks is provided in the supplementary material.

3.2. Benchmark details

This section standardizes the conditions used by our benchmark to compare different pretext tasks. Further explanation for using these conditions are outlined in the supplementary.
Datasets: We experiment with two different dataset types, 1) where appearance is more important, and 2) where time is more important. For appearance based, we use Kinetics-400 [35], UCF101 [67], and HMDB51 [40], where appearance is more important (recognize activity with a single frame) than temporal aspect, and for temporal aspect, we use Something Something-V2 [24] and Diving48 [45], where temporal information plays a significant role (require few frames to recognize activity). More details are in the supplementary.
Spatio-temporal architectures: We consider three different network capacities, 1) small-capacity, 2) medium-capacity, and large-capacity. For small capacity networks, we use ShuffleNet V1 2.0X [89], whereas for medium capacity we focus on R(2+1)D [75] (R21D). We do not include large capacity networks in our main benchmark in the interest of computational efficiency; additional results for such a model, VideoSwin [47] is shown in the supplementary.
Downstream tasks: We show results and analysis on two different downstream tasks - *action recognition* and *clip retrieval*. These two tasks are the most prominent in the field of self-supervised learning in videos. Full finetuning is performed as opposed to linear probing to adapt models.
Evaluation and Analysis: We use top-1 accuracy for action recognition and top-K for Clip retrieval. For robustness performance, we calculate the relative robustness score (R_s) using original accuracy on clean test set (A_c) and perturbed accuracy on noisy test set (A_p) as $R_s = \frac{A_c - A_p}{A_c}$. Centered Kernel alignment (CKA) [51] maps illustrates model behaviours. More details in supplementary.

4. Benchmark Analysis

In this section, we perform analysis across the following five aspects:
Effect of Pretraining Dataset Size: In self-supervised learning, a fundamental question is whether the size of the pretraining dataset influences downstream task performance. It is crucial to determine if increasing the dataset size leads to proportional improvements in performance. Additionally, a common trend in SSL is to train models for extended durations during pretraining. We investigate whether prolonged training meaningfully contributes to performance gains. To address these questions, we analyze different training stages across multiple architectures and pretext tasks.
Impact of Task Complexity: Previous studies suggest that increasing task complexity enhances representation learning,
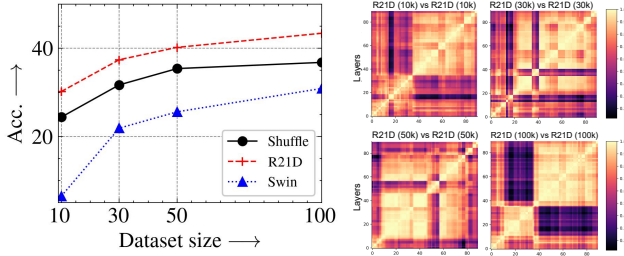
Figure 2. Left: **Dataset subset** performance for three different architectures on RSPNet pretext task (x-axis: subset size, y-axis: Top-1 Accuracy). Here, 10 means 10k dataset subset, 30 means 30k, and so on. Right: **CKA maps** for RSPNet on different subsets with R21D backbone.

whereas reducing complexity may lead to suboptimal solutions. We examine this hypothesis in detail by evaluating multiple tasks across different model architectures to assess how complexity influences learned representations.

Effect of Data Distribution: Most existing self-supervised methods evaluate performance on Kinetics-400 (K400) and UCF101, both of which exhibit strong appearance bias. However, we focus on datasets where temporal dynamics play a crucial role, such as Something-Something v2 (SSv2) and Diving48. This allows us to better understand the generalization of self-supervised methods beyond appearance-driven cues.

Robustness of SSL Tasks: We assess the robustness of SSL methods against data noise [28], examining which factors contribute to their stability under domain shifts. Understanding these aspects is critical for developing more resilient self-supervised learning approaches.

Feature Analysis: Finally, we analyze the learned feature space to determine whether representations are complementary when models are trained under different protocols. This helps uncover how different pretext tasks and training conditions influence feature learning and transferability.

4.1. Effect of dataset-size

We begin by analyzing the impact of pretraining dataset size variation. The network is trained on four subsets of Kinetics-400 (K400): 10k, 30k, 50k, and 100k videos, ensuring that the number of videos per class remains consistent across subsets. Each smaller pretraining dataset is a strict subset of the larger one (i.e., $10k \subset 30k \subset 50k \subset 100k$). We examine three key aspects related to the dependence on pretraining subset size: a) how different pretext tasks behave as the pretraining dataset size increases, b) performance variations across different backbone capacities, and c) the effect of training duration across different pretext tasks.

Observations: As shown in Table 1, we observe that except for TDL, all pretext tasks exhibit performance improvements with an increase in pretraining dataset size. When analyzing specific pretext task transformation categories (Table 1),

we find that *spatio-temporal* tasks benefit the most from increased data, achieving a performance gain of approximately 13%, whereas *temporal* tasks show the least improvement, with only a 3% gain. Regarding training duration (Table 2), performance gains become marginal (<1.5%) after 100 epochs, indicating diminishing returns from extended training. Comparing contrastive and non-contrastive approaches, contrastive methods exhibit an average improvement of 1% beyond 100 epochs, while non-contrastive tasks achieve a more significant gain of approximately 5

Inference: (i) *Spatio-temporal pretext tasks exhibit the highest performance gains with an increase in dataset size, as they rely on transformations across both spatial (appearance) and temporal (motion) dimensions, making them more dependent on larger datasets compared to other tasks.* (ii) *Contrastive tasks converge faster than non-contrastive ones, reaching their optimal performance in a relatively shorter training duration.*

4.2. Impact of change in task complexity

Next, we examine the impact of task complexity, focusing exclusively on non-contrastive tasks, as defining complexity for contrastive-based approaches is non-trivial. We evaluate three levels of complexity (C1, C2, C3) for each task: a) *RotNet*: Varying the number of rotation angles from 2 to 4, b) *VCOP*: Increasing the number of shuffled clips from 3 to 5, and c) *PRP*: Modifying the dilation sampling rates from 2 to 4 classes. We aim to address two key questions: 1) Does increasing task complexity lead to better spatio-temporal feature learning during pretraining? 2) Does model capacity influence the effectiveness of task complexity?

Observations: From Table 3, we observe that increasing task complexity does not always lead to improved performance. For example, ShuffleNet exhibits minimal improvement or even performance degradation with increased task complexity. CKA maps reveal a transition from staggered grid-like structures to multi-block patterns, indicating saturation as complexity increases. Among different transformation categories, performance gains from increased complexity are more evident in larger models, particularly for *spatio-temporal* tasks. Comparing ShuffleNet and R21D, we find that R21D produces more structured feature representations, while ShuffleNet results in dark block patterns, suggesting that larger models retain the ability to learn richer representations. Additional CKA maps are provided in the supplementary materials.

Inference: (i) *An increase in pretext task complexity does not always translate to better spatio-temporal feature learning. Its effectiveness depends on both the task itself and the model's capacity.* (ii) *If higher complexity leads to improved feature learning, the model must also have sufficient capacity; otherwise, the task becomes too challenging, preventing the model from learning meaningful representations.*

Table 1. Evaluation of different pretext tasks on **different subset size** on R21D network (%).

	Non-Contrastive			Contrastive		
Subset	Rot	VCOP	PRP	CVRL	TDL	RSPNet
10k	37.6	46.3	17.5	55.9	31.1	70.9
30k	36.2	50.4	42.7	56.9	30.9	76.4
50k	41.2	51.5	46.2	61.2	30.2	78.0

Table 2. **Performance at different stages** of training for all pretext tasks on R21D (50k)(%).

	Non-Contrastive			Contrastive		
Epochs	Rot	VCOP	PRP	CVRL	TDL	RSPNet
50	35.4	52.2	24.1	55.7	32.1	75.0
100	37.3	52.3	34.8	58.5	31.3	76.1
150	40.7	51.3	46.7	60.2	31.5	76.5
200	40.9	52.8	45.0	60.5	30.2	77.4

Table 3. **Complexity Variation.** TC: Task complexity. Results are shown on UCF101 with ShuffleNet/R21D backbone.

TC↓	S	T	ST
C1	20.1/48.3	41.6/**56.8**	**24.2**/38.9
C2	**20.2/58.3**	**41.8**/54.8	18.1/44.4
C3	16.6/41.2	40.6/55.6	21.9/**46.2**

	Non-Contrastive			Contrastive			
	Rot	VCOP	PRP	CVRL	TDL	RSP	Avg.
R21D	10.7	19.0	70.1	78.4	26.7	68.8	45.6
Shuffle	28.3	28.4	22.8	51.9	43.5	28.6	33.9

Table 4. **Robustness analysis** on the relative decrease in % performance across different pretext tasks on noisy UCF101 dataset. The performance is averaged over 4 noises.

(a) UCF101   (b) DV48

Figure 3. **Effect of different dataset distributions:** Here, S, T, and ST mean spatial(CVRL), temporal(VCOP), and, spatio-temporal(RSPNet) respectively. X-axis shows *source* dataset and Y-axis shows Top-1 accuracy.

4.3. Effect of dataset distribution

Shifting our focus to datasets with stronger temporal cues, we extend our experiments by pretraining on SSv2 and fine-tuning on Diving48. We aim to address two key questions: a) Does the categorization of pretext tasks influence performance across *source* (pretraining) and *target* (downstream) datasets? b) How does the choice of *source* dataset impact pretext tasks that focus exclusively on either *spatial* or *temporal* learning?

Observations: From Figure 3, we observe that *spatio-temporal* pretext tasks consistently outperform others on both downstream datasets, UCF101 and Diving48, with margins of 15-40Comparing spatial and temporal pretext tasks, we find that their performance is highly dependent on the *source* dataset. As shown in Figure 3, both tasks perform better when the *source* dataset shares similar properties with the features the pretext task is designed to learn. Furthermore, spatial pretext tasks exhibit a stronger dependence on the *source* dataset, as evidenced by the significant performance drop for CVRL—40% on UCF101 and 30% on Diving48—when pretrained on SSv2 instead of K400. In contrast, temporal pretext tasks experience smaller performance drops of 15% and 10%, respectively, when pretrained on K400 instead of SSv2.

Inference: (i) *Spatio-temporal pretext tasks learn more generalizable features, making them less dependent on source and target data distributions.* (ii) *Spatial and temporal pretext tasks are more effective when the source dataset aligns with their respective learning objectives.* (iii) *Temporal pretext tasks perform well when the target dataset has strong temporal dependencies, whereas spatial tasks rely more heavily on the source data distribution.*
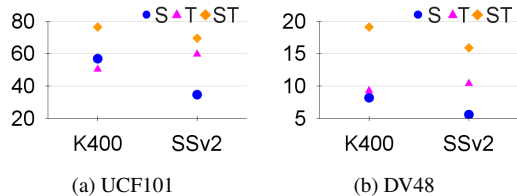
4.4. Robustness of SSL tasks

Similar to out-of-distribution (OOD) datasets, the introduction of noise alters the data distribution, impacting model performance. We evaluate models under various types of noise introduced in [63] with different severity levels, using the UCF101 test dataset. Specifically, we examine four appearance-based noise types: Gaussian, Shot, Impulse, and Speckle [28]. Our analysis focuses on two key aspects: a) How robust are different categories of pretext tasks to noise? b) Does the network architecture influence robustness against noise in the dataset? In the main paper, we discuss results for a single severity level, while a comprehensive analysis across multiple severity levels is provided in the supplementary material.

Observations: As shown in Table 4, contrastive tasks exhibit a larger relative drop in performance compared to non-contrastive tasks across both R21D and ShuffleNet backbones. Among the models analyzed, RotNet-R21D demonstrates the highest robustness, with a 10.7% relative decrease, whereas PRP-R21D shows the highest vulnerability, experiencing a 70.1% drop in performance.

Inference: *Contrastive approaches are less robust to noise as compared with non-contrastive.*

4.5. Feature analysis

We further analyze the features learned by different pretext tasks under various configurations, with a particular focus on their complementary nature. To study this, we employ knowledge distillation [16], leveraging the principle that knowledge distilled from an ensemble of teacher networks enhances the performance of a student model.
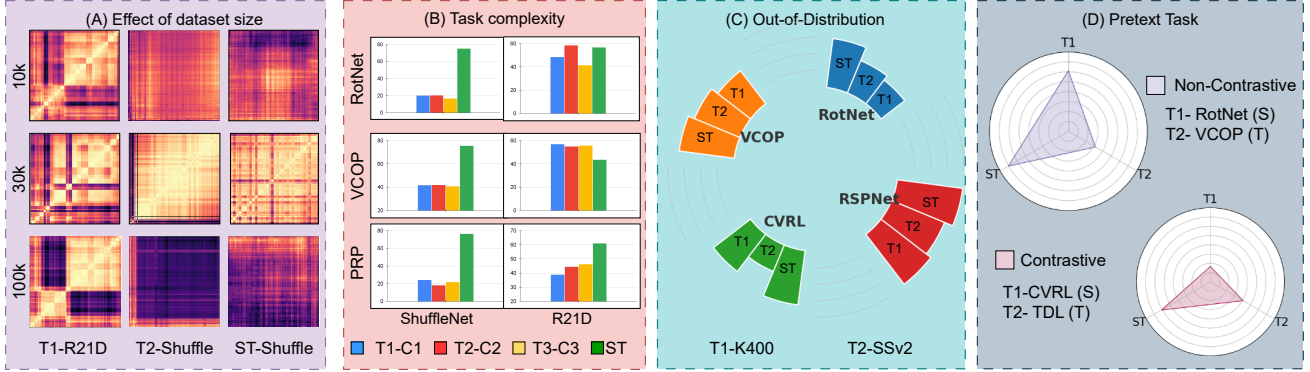
Figure 4. **Feature analysis overview.** This figure shows how KD as a tool is beneficial across multiple scenarios. Brief details for each setup (Left to right): (A) *Effect of dataset size:* Teachers (T1 and T2) are different architectures for a single subset. Student model (ST-Shuffle) CKA maps shows it learns complementary information especially for 30k. (B) *Task Complexity:* Teachers are multiple complexities across the same task. (C1, C2, C3 - different complexities as teachers.) We observe in most of the scenarios, Student (ST) networks outperforms all teacher models which proves learning of orthogonal information from multiple teachers. (C) *Out-of-Distribution:* Models from different *source* datasets are teachers. Student model (ST) outperforms both teachers trained on two different datasets. (D) *Pretext Tasks:* Spatial and temporal task networks are teachers, and, student model (ST) learnt from two different categories of pretext tasks - spatial and temporal incorporate knowledge from both and outperforms both of the teachers for both contrastive and non-contrastive.

The multi-teacher knowledge distillation loss is defined as: $\mathcal{L}_{KD} = \mathcal{L}_{CE} + \mathcal{L}_{KL_1} + \mathcal{L}_{KL_2} + ... + \mathcal{L}_{KL_n}$ where $\mathcal{L}_{CE}$ is the cross-entropy loss for hard labels, and $\mathcal{L}_{KL_n}$ represents the KL-divergence loss from teacher n. We investigate the transfer of complementary information by using our benchmark models as teachers in different combinations across four key axes: 1) Different architectures as teachers within the same *dataset size*, 2) Teachers with varying complexities within a pretext task, 3) Models trained on multiple *source* datasets, and 4) The same architecture trained on multiple pretext tasks. Figure 4 provides a summary of the key *observations* for each aspect, with further details in the supplementary material.

Observations: Although teacher network performance improves with an increase in dataset subset size, the gain in complementary information diminishes beyond 30k samples (Figs. 5(a) & 5(b)). However, knowledge distillation significantly reduces training time while improving performance, as seen in Fig. 4(a). Regardless of the pretext task category, smaller architectures benefit more from complementary information and often outperform their teacher models. In contrast, larger architectures show task-dependent improvements. Moreover, across both transformation-based and contrastive tasks, knowledge distillation from multiple *source* datasets enhances feature learning and results in superior student model performance. Finally, student networks consistently outperform standalone spatio-temporal models in both contrastive and non-contrastive domains.

Inference: (i) *Knowledge can be effectively distilled across different architectures for a given dataset subset size (Fig. 4 (a)).* (ii) *Leveraging multiple source datasets in-*

troduces complementary information, leading to improved learning (Fig. 4 (c)). (iii) *Pretext tasks from different categories learn orthogonal features, contributing to a more diverse and enriched representation space (Fig. 4 (d)).*

5. Lessons Learned

Our analysis across different axes reveals several key insights: (i) Contrastive tasks exhibit faster learning but are highly susceptible to noise. (ii) Increasing dataset size or task complexity does not significantly improve the learning of spatio-temporal features in smaller models; however, the features learned are more robust to noise. (iii) Temporal tasks are inherently more challenging to learn, as performance gains remain minimal even with increased training time, dataset size, or task complexity, indicating the intrinsic difficulty of these tasks. (iv) Spatio-temporal pretext tasks benefit from increased dataset size and task complexity (provided the model capacity allows), and their ability to learn meaningful spatio-temporal features remains independent of data distribution. Building upon these findings, we further analyze the learned feature space to understand how models acquire orthogonal information within each comparison axis. Based on these insights, we investigate strategies to enhance performance on downstream tasks, specifically action classification and clip retrieval.

Clip retrieval For this downstream task, we generate feature vectors using pretrained weights and retrieve the nearest neighbor by computing the cosine distance between test and train feature vectors. We conduct our analysis on UCF101 and HMDB51 with different *source* data distributions: K400 and SSv2. *Observations:* The spatio-temporal pretext task consistently outperforms other categories, independent of
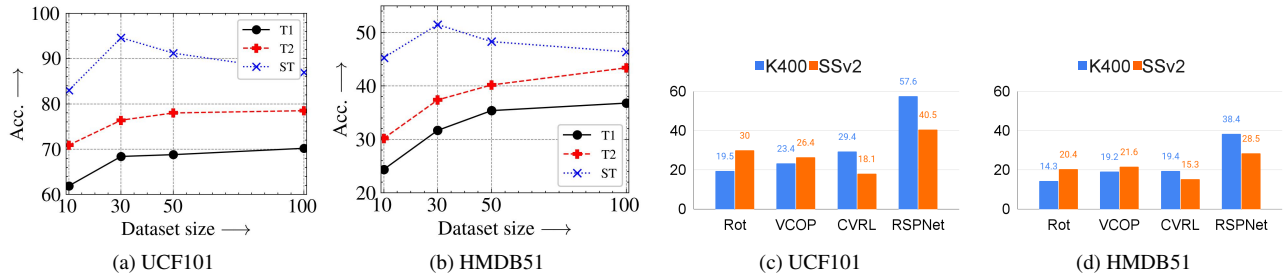
Figure 5. **Knowledge distillation** using teachers trained on multiple subset sizes on RSPNet. Student: ShuffleNet a) UCF101 and b) HMDB51. Here T1 is Teacher-1 (shufflenet) and T2 is teacher-2 (R21D). **Top@5 Clip Retrieval** - R21D on c) UCF101 and d) HMDB51, pre-trained on K400 and SSv2 - 30k subset.

Table 5. **Comparison with previous approaches** pre-trained on K400. Ours (* best performing) is RSPNet pretrained on 30k subset of K400. † - Different pre-training data. (%)

Approach	Venue	NxW/H	Backbone	Pre-training	UCF101	HMDB51
Generative						
VIMPAC [70]	-	10x256	ViT-L	HTM	92.7	65.9
VideoMAE [73]	NeurIPS'22	16x224	ViT-B	K400	91.3	62.6
MME [69]	CVPR'23	16x224	ViT-B	K400	96.5	78.0
MVD [80]	CVPR'23	16x224	ViT-B	IN1K+K400	97.0	76.4
EVEREST [30]	-	16x224	ViT-B	-	93.4	68.1
SCE [15]	WACV'23	16x224	ResNet3D-50	K400	95.3	74.7
Context						
PacePred [83]	ECCV'20	16x112	R21D-18	K400	77.1	36.6
TempTrans [32]	ECCV'20	16x112	R3D-18	K400	79.3	49.8
STS [79]	TPAMI-21	16x112	R21D-18	K400	77.8	40.5
VideoMoCo [53]	CVPR'21	16x112	R21D-18	K400	78.7	49.2
RSPNet [10]	AAAI'21	16x112	R21D-18	K400	81.1	44.6
TaCo [6]	-	16x224	R21D-18	K400	81.8	46.0
TCLR [13]	CVIU'22	16x112	R21D-18	K400	88.2	60.0
CVRL [56]	CVPR'21	32x224	R21D-18	K400	92.9	67.9
TransRank [17]	CVPR'22	16x112	R21D-18	K200	87.8	60.1
Multi-Modal						
AVTS [39]	NeurIPS'18	25x224	I3D	K400	83.7	53.0
GDT [54] †	-	32x112	R21D	IG65M	95.2	72.8
XDC [4]	NeurIPS'20	32x224	R21D	K400	84.2	47.1
Ours *	-	16x112	R21D-18	K400-30k	97.3	51.5

the *source* data distribution, aligning with our earlier findings. Contrastive learning excels at capturing *appearance* features during pretraining, which is advantageous since both downstream datasets are *appearance*-centric. Temporal tasks exhibit comparable performance regardless of the *source* dataset used for pretraining. This suggests that, even when trained on an appearance-based dataset, temporal tasks do not overly rely on spatial features.

Action Classification For this task, we fine-tune the model end-to-end on the UCF101 and HMDB51 datasets. As shown in Table 5, our best-performing model is obtained through knowledge distillation, as discussed in the previous section. The results demonstrate that our model surpasses prior state-of-the-art methods. *Observations:* Despite being trained on only 30k videos—significantly fewer than the 200k+ videos used by other pretext tasks—our model achieves superior performance on UCF101, outperforming

both single- and multi-modal approaches by a substantial margin. On HMDB51, our model achieves competitive performance with a classification accuracy of 51.5%.

5.1. Surprising Findings

We have multiple inferences from different axes of analysis. However, to club a few which are new and helpful for video self-supervised community, we list down those here:

Dataset Size and Training Time Dependency: Contrary to the conventional belief that extensive training data is essential for achieving optimal performance, our findings reveal that beyond a certain threshold, additional data yields diminishing returns for self-supervised learning (SSL). This insight has significant implications, as it enables a substantial reduction in training data requirements while achieving nearly a 10× reduction in training time—particularly beneficial for computationally intensive video processing tasks.

Table 6. **Analysis on ViFMs**. Zero-shot classification accuracy on UCF-101. I:Image, V: Video.

ViFM	Type.	Pretraining Data	Frames x Rate	Accuracy
ViFi-CLIP [60]	I	K-400	32 x 2	77.3
X-CLIP [52]	I	K-400	8 x 8	71.6
EZ-CLIP [2]	I	K-400	8 x 8	70.5
ViCLIP [82]	V	InternVid-10M	8 x 8	75.5
LanguageBind [90]	V	VIDAL-10M	8 x 8	69.9

Table 7. **Knowledge Distillation** between different ViFM pairs as teachers, and R21D as the student.

ViFM	X-CLIP	ViFi-CLIP	EZ-CLIP	ViCLIP	LanguageBind
X-CLIP	X	83.2	88.7	88.2	87.6
ViFi-CLIP	X	X	88.0	86.6	86.6
EZ-CLIP	X	X	X	85.0	86.9
ViCLIP	X	X	X	X	85.4
LanguageBind	X	X	X	X	X

Moreover, we demonstrate that knowledge distillation (KD) can outperform the original approach trained on 100% of the data while utilizing only 10% of it, thereby optimizing resource utilization by approximately 80%.

Robustness to Real-World Noise: Surprisingly, contrastive tasks exhibit greater susceptibility to noise compared to non-contrastive tasks. Additionally, in certain scenarios, smaller networks demonstrate higher robustness than larger networks. We believe these findings are novel, as no prior work in the community has systematically explored these aspects. This insight is particularly valuable for real-world deployments where robustness is a critical requirement.

Complementary Knowledge: The performance improvements achieved through KD from different data distributions and pretext task categories highlight a promising direction for a new SSL paradigm. Specifically, a multi-teacher, multi-student framework, where each teacher specializes in either spatial or temporal tasks and is trained on a diverse set of data sources, could provide an effective learning strategy. Our analysis suggests that such an approach would enhance feature learning and task generalization.

5.2. Recommendations

Based on our findings, we propose the following recommendations for designing effective SSL strategies:

1. *Training Speed:* If pretraining time is a constraint, contrastive tasks can accelerate the learning process. However, they may be less robust to noise.
2. *Data Distribution:* When possible, a spatio-temporal pretext task should be preferred, as it generalizes well across data distributions. If this is not feasible, the pretext task should align with the characteristics of the pretraining dataset.
3. *Model Capacity:* If the model has limited capacity, increasing the pretraining dataset size or using complex pretext tasks will not yield significant benefits.
4. *Robustness:* For applications requiring high robustness, non-contrastive pretext tasks should be favored over contrastive ones.
5. *Performance:* Pretext tasks learn complementary features across model architectures, pretraining datasets, task categories, and task complexities. This complementary knowledge can be distilled to develop stronger spatio-temporal feature representations.

5.3. Extension of Findings to Video Foundation Models (ViFMs)

We extend our study to Video Foundation Models (ViFMs) (Tables 6 and 7). Our analysis includes both image-based ViFMs—such as EZ-CLIP, X-CLIP, and ViFi-CLIP—which are adapted from image foundation models, as well as video-based ViFMs—such as LanguageBind and ViCLIP—which are trained from scratch on videos. Notably, all ViFMs utilize contrastive pretraining objectives.

Dataset Size: Increasing dataset size or complexity does not necessarily enhance the ability of smaller models to learn better spatio-temporal features (Table 6). Notably, ViCLIP and LanguageBind, despite being pretrained on significantly larger datasets, underperform compared to models trained on the smaller Kinetics-400 dataset. Furthermore, simply increasing the number of frames during training yields better performance than relying solely on larger pretraining datasets.

Complementary Knowledge: The performance improvements observed with KD from different ViFMs suggest a promising strategy for training a new foundational model. This approach involves a multi-teacher, multi-student framework, where each teacher is a ViFM pretrained under different conditions—varying data sources, multi-stage pretraining strategies, and distinct pretraining objectives. Our analysis (Table 7) indicates that such a framework would foster a more effective learning process.

6. Conclusion

In this study, we systematically analyze various factors influencing self-supervised learning in the video domain. We establish a benchmark that provides an intuitive categorization of pretext tasks, enabling a more structured comparison across different learning paradigms. To the best of our knowledge, such an in-depth exploration of self-supervised learning for video understanding has not been previously conducted. Our findings uncover several key insights that pave the way for future research directions. Additionally, we demonstrate the practical impact of these insights by achieving state-of-the-art performance on video action recognition while utilizing only 10% of the pretraining dataset compared to existing methods. We believe this benchmark study will serve as a valuable resource for the research community, fostering a deeper understanding of self-supervised learning in the video domain.

References

[1] Triantafyllos Afouras, Andrew Owens, Joon Son Chung, and Andrew Zisserman. Self-supervised learning of audio-visual objects from video. *ArXiv*, abs/2008.04237, 2020. 2

[2] Shahzad Ahmad, Sukalpa Chanda, and Yogesh S Rawat. Ez-clip: Efficient zeroshot video action recognition. *arXiv preprint arXiv:2312.08010*, 2023. 8

[3] Unaiza Ahsan, Rishi Madhok, and Irfan A. Essa. Video jigsaw: Unsupervised learning of spatiotemporal context for video action recognition. *CoRR*, abs/1808.07507, 2018. 2

[4] Humam Alwassel, Dhruv Kumar Mahajan, Lorenzo Torresani, Bernard Ghanem, and Du Tran. Self-supervised learning by cross-modal audio-video clustering. *ArXiv*, abs/1911.12667, 2020. 7, 8

[5] Anurag Arnab, Mostafa Dehghani, Georg Heigold, Chen Sun, Mario Lucic, and Cordelia Schmid. Vivit: A video vision transformer. *ArXiv*, abs/2103.15691, 2021. 2

[6] Yutong Bai, Haoqi Fan, Ishan Misra, Ganesh Venkatesh, Yongyi Lu, Yuyin Zhou, Qihang Yu, Vikas Chandra, and Alan Loddon Yuille. Can temporal information help with contrastive self-supervised learning? *ArXiv*, abs/2011.13046, 2020. 7, 8

[7] Sagie Benaim, Ariel Ephrat, Oran Lang, Inbar Mosseri, William T. Freeman, Michael Rubinstein, Michal Irani, and Tali Dekel. Speednet: Learning the speediness in videos. In *Proceedings of the IEEE/CVF Conference on Computer Vision and Pattern Recognition (CVPR)*, 2020. 2

[8] Gedas Bertasius, Heng Wang, and Lorenzo Torresani. Is space-time attention all you need for video understanding? *ArXiv*, abs/2102.05095, 2021. 2

[9] J. Carreira, Eric Noland, Chloe Hillier, and Andrew Zisserman. A short note on the kinetics-700 human action dataset. *ArXiv*, abs/1907.06987, 2019. 5

[10] Peihao Chen, Deng Huang, Dongliang He, Xiang Long, Runhao Zeng, Shilei Wen, Mingkui Tan, and Chuang Gan. Rspnet: Relative speed perception for unsupervised video representation learning. In *AAAI*, 2021. 1, 2, 3, 7, 8

[11] Ting Chen, Simon Kornblith, Mohammad Norouzi, and Geoffrey E. Hinton. A simple framework for contrastive learning of visual representations. *ArXiv*, abs/2002.05709, 2020. 3

[12] Jinwoo Choi, Chen Gao, Joseph C.E. Messou, and Jia-Bin Huang. Why can't i dance in the mall? learning to mitigate scene bias in action recognition. In *NeurIPS*, 2019. 3

[13] I. Dave, Rohit Gupta, M. N. Rizve, and M. Shah. Tclr: Temporal contrastive learning for video representation. *ArXiv*, abs/2101.07974, 2021. 1, 2, 7, 8

[14] Ishan Dave, Zacchaeus Scheffer, Akash Kumar, Sarah Shiraz, Yogesh Singh Rawat, and Mubarak Shah. Gabriellav2: Towards better generalization in surveillance videos for action detection. In *Proceedings of the IEEE/CVF Winter Conference on Applications of Computer Vision (WACV) Workshops*, pages 122–132, 2022. 2

[15] Julien Denize, Jaonary Rabarisoa, Astrid Orcesi, Romain Hérault, and Stéphane Canu. Similarity contrastive estimation for self-supervised soft contrastive learning. In *Proceedings of the IEEE/CVF Winter Conference on Applications of Computer Vision (WACV)*, pages 2706–2716, 2023. 7

[16] Shangchen Du, Shan You, Xiaojie Li, Jianlong Wu, Fei Wang, Chen Qian, and Changshui Zhang. Agree to disagree: Adaptive ensemble knowledge distillation in gradient space. In *Advances in Neural Information Processing Systems*, pages 12345–12355. Curran Associates, Inc., 2020. 5

[17] Haodong Duan, Nanxuan Zhao, Kai Chen, and Dahua Lin. Transrank: Self-supervised video representation learning via ranking-based transformation recognition. *2022 IEEE/CVF Conference on Computer Vision and Pattern Recognition (CVPR)*, pages 2990–3000, 2022. 2, 7, 8

[18] Haoqi Fan, Bo Xiong, Karttikeya Mangalam, Yanghao Li, Zhicheng Yan, Jitendra Malik, and Christoph Feichtenhofer. Multiscale vision transformers. *ArXiv*, abs/2104.11227, 2021. 2

[19] Christoph Feichtenhofer, Haoqi Fan, Bo Xiong, Ross B. Girshick, and Kaiming He. A large-scale study on unsupervised spatiotemporal representation learning. *2021 IEEE/CVF Conference on Computer Vision and Pattern Recognition (CVPR)*, pages 3298–3308, 2021. 3

[20] Basura Fernando, Hakan Bilen, E. Gavves, and Stephen Gould. Self-supervised video representation learning with odd-one-out networks. *2017 IEEE Conference on Computer Vision and Pattern Recognition (CVPR)*, pages 5729–5738, 2017. 2

[21] Aaryan Garg, Akash Kumar, and Yogesh S Rawat. Stpro: Spatial and temporal progressive learning for weakly supervised spatio-temporal grounding. *arXiv preprint arXiv:2502.20678*, 2025. 2

[22] Jianping Gou, B. Yu, Stephen J. Maybank, and Dacheng Tao. Knowledge distillation: A survey. *ArXiv*, abs/2006.05525, 2021. 1

[23] Priya Goyal, Dhruv Mahajan, Abhinav Gupta, and Ishan Misra. Scaling and benchmarking self-supervised visual representation learning. *arXiv preprint arXiv:1905.01235*, 2019. 2

[24] Raghav Goyal, Samira Ebrahimi Kahou, Vincent Michalski, Joanna Materzynska, Susanne Westphal,

Heuna Kim, Valentin Haenel, Ingo Fründ, Peter N. Yianilos, Moritz Mueller-Freitag, Florian Hoppe, Christian Thurau, Ingo Bax, and Roland Memisevic. The "something something" video database for learning and evaluating visual common sense. *2017 IEEE International Conference on Computer Vision (ICCV)*, pages 5843–5851, 2017. 3, 2

[25] Sheng Guo, Zihua Xiong, Yujie Zhong, Limin Wang, Xiaobo Guo, Bing Han, and Weilin Huang. Cross-architecture self-supervised video representation learning. *2022 IEEE/CVF Conference on Computer Vision and Pattern Recognition (CVPR)*, pages 19248–19257, 2022. 2

[26] Tengda Han, Weidi Xie, and Andrew Zisserman. Memory-augmented dense predictive coding for video representation learning. In *European Conference on Computer Vision*, 2020. 1

[27] K. Hara, H. Kataoka, and Y. Satoh. Learning spatio-temporal features with 3d residual networks for action recognition. *2017 IEEE International Conference on Computer Vision Workshops (ICCVW)*, pages 3154–3160, 2017. 1, 2

[28] Dan Hendrycks and Thomas G. Dietterich. Benchmarking neural network robustness to common corruptions and perturbations. *ArXiv*, abs/1903.12261, 2019. 4, 5

[29] De-An Huang, Vignesh Ramanathan, Dhruv Mahajan, Lorenzo Torresani, Manohar Paluri, Li Fei-Fei, and Juan Carlos Niebles. What makes a video a video: Analyzing temporal information in video understanding models and datasets. In *2018 IEEE/CVF Conference on Computer Vision and Pattern Recognition*, pages 7366–7375, 2018. 3

[30] Sunil Hwang, Jaehong Yoon, Youngwan Lee, and Sung Ju Hwang. Efficient video representation learning via motion-aware token selection. *arXiv preprint arXiv:2211.10636*, 2022. 7

[31] Forrest N. Iandola, Song Han, Matthew W. Moskewicz, Khalid Ashraf, William J. Dally, and Kurt Keutzer. Squeezenet: Alexnet-level accuracy with 50x fewer parameters and <0.5mb model size, 2016. cite arxiv:1602.07360Comment: In ICLR Format. 2

[32] S. Jenni, Givi Meishvili, and P. Favaro. Video representation learning by recognizing temporal transformations. *ArXiv*, abs/2007.10730, 2020. 2, 7, 8

[33] L. Jing and Y. Tian. Self-supervised visual feature learning with deep neural networks: A survey. *IEEE Transactions on Pattern Analysis and Machine Intelligence*, pages 1–1, 2020. 1, 2

[34] Longlong Jing, Xiaodong Yang, Jingen Liu, and Y. Tian. Self-supervised spatiotemporal feature learning via video rotation prediction. *arXiv: Computer Vision and Pattern Recognition*, 2018. 1, 3

[35] W. Kay, J. Carreira, K. Simonyan, Brian Zhang, Chloe Hillier, Sudheendra Vijayanarasimhan, F. Viola, T. Green, T. Back, A. Natsev, Mustafa Suleyman, and Andrew Zisserman. The kinetics human action video dataset. *ArXiv*, abs/1705.06950, 2017. 3, 2

[36] Dahun Kim, Donghyeon Cho, and In So Kweon. Self-supervised video representation learning with space-time cubic puzzles. *Proceedings of the AAAI Conference on Artificial Intelligence*, 33(01):8545–8552, 2019. 2

[37] A. Kolesnikov, X. Zhai, and L. Beyer. Revisiting self-supervised visual representation learning. In *2019 IEEE/CVF Conference on Computer Vision and Pattern Recognition (CVPR)*, pages 1920–1929, 2019. 3

[38] Okan Köpüklü, Neslihan Kose, Ahmet Gunduz, and Gerhard Rigoll. Resource efficient 3d convolutional neural networks. In *2019 IEEE/CVF International Conference on Computer Vision Workshop (ICCVW)*, pages 1910–1919. IEEE, 2019. 2

[39] Bruno Korbar, Du Tran, and Lorenzo Torresani. Co-operative learning of audio and video models from self-supervised synchronization. In *NeurIPS*, 2018. 7, 8

[40] H. Kuehne, H. Jhuang, E. Garrote, T. Poggio, and T. Serre. Hmdb: A large video database for human motion recognition. In *2011 International Conference on Computer Vision*, pages 2556–2563, 2011. 3, 2

[41] Akash Kumar and Yogesh Singh Rawat. End-to-end semi-supervised learning for video action detection. In *Proceedings of the IEEE/CVF Conference on Computer Vision and Pattern Recognition (CVPR)*, 2022. 2

[42] Akash Kumar, Ashlesha Kumar, Vibhav Vineet, and Yogesh Singh Rawat. Benchmarking self-supervised video representation learning. *Neural Information Processing Systems 4th Workshop on Self-Supervised Learning: Theory and Practice*, 2023. 3

[43] Akash Kumar, Zsolt Kira, and Yogesh Singh Rawat. Contextual self-paced learning for weakly supervised spatio-temporal video grounding. *Proceedings of the International Conference on Learning Representations (ICLR)*, 2025. 2

[44] Akash Kumar, Sirshapan Mitra, and Yogesh Singh Rawat. Stable mean teacher for semi-supervised video action detection. *Proceedings of the AAAI Conference on Artificial Intelligence*, 2025. 2

[45] Yingwei Li, Yi Li, and Nuno Vasconcelos. Resound: Towards action recognition without representation bias. In *ECCV*, 2018. 3, 2

[46] Ze Liu, Yutong Lin, Yue Cao, Han Hu, Yixuan Wei, Zheng Zhang, Stephen Lin, and Baining Guo. Swin transformer: Hierarchical vision transformer using

shifted windows. *2021 IEEE/CVF International Conference on Computer Vision (ICCV)*, pages 9992–10002, 2021. 2

[47] Ze Liu, Jia Ning, Yue Cao, Yixuan Wei, Zheng Zhang, Stephen Lin, and Han Hu. Video swin transformer. *2022 IEEE/CVF Conference on Computer Vision and Pattern Recognition (CVPR)*, pages 3192–3201, 2022. 3, 2

[48] Dezhao Luo, Chang Liu, Y. Zhou, Dongbao Yang, Can Ma, Qixiang Ye, and Weiping Wang. Video cloze procedure for self-supervised spatio-temporal learning. *ArXiv*, abs/2001.00294, 2020. 2

[49] I. Misra, C. L. Zitnick, and M. Hebert. Unsupervised learning using sequential verification for action recognition. *ArXiv*, abs/1603.08561, 2016. 2

[50] Rajat Modi, Aayush Jung Rana, Akash Kumar, Praveen Tirupattur, Shruti Vyas, Yogesh Singh Rawat, and Mubarak Shah. Video action detection: Analysing limitations and challenges. *2022 IEEE/CVF Conference on Computer Vision and Pattern Recognition Workshops (CVPRW)*, pages 4907–4916, 2022. 2

[51] Thao Nguyen, Maithra Raghu, and Simon Kornblith. Do wide and deep networks learn the same things? uncovering how neural network representations vary with width and depth. *ArXiv*, abs/2010.15327, 2021. 3

[52] Bolin Ni, Houwen Peng, Minghao Chen, Songyang Zhang, Gaofeng Meng, Jianlong Fu, Shiming Xiang, and Haibin Ling. Expanding language-image pretrained models for general video recognition. In *European Conference on Computer Vision*, pages 1–18. Springer, 2022. 8

[53] Tian Pan, Yibing Song, Tianyu Yang, Wenhao Jiang, and Wei Liu. Videomoco: Contrastive video representation learning with temporally adversarial examples. *2021 IEEE/CVF Conference on Computer Vision and Pattern Recognition (CVPR)*, pages 11200–11209, 2021. 1, 7, 8

[54] Mandela Patrick, Yuki M. Asano, Ruth Fong, João F. Henriques, Geoffrey Zweig, and Andrea Vedaldi. Multi-modal self-supervision from generalized data transformations. *ArXiv*, abs/2003.04298, 2020. 7, 8

[55] Senthil Purushwalkam and Abhinav Gupta. Pose from action: Unsupervised learning of pose features based on motion. *arXiv preprint arXiv:1609.05420*, 2016. 2

[56] Rui Qian, Tianjian Meng, Boqing Gong, Ming-Hsuan Yang, H. Wang, Serge J. Belongie, and Yin Cui. Spatiotemporal contrastive video representation learning. *2021 IEEE/CVF Conference on Computer Vision and Pattern Recognition (CVPR)*, pages 6960–6970, 2021. 1, 2, 3, 7, 8

[57] Aayush Rana and Yogesh Rawat. Are all frames equal? active sparse labeling for video action detection. In

[58] Aayush J. Rana and Yogesh S. Rawat. Hybrid active learning via deep clustering for video action detection. In *Proceedings of the IEEE/CVF Conference on Computer Vision and Pattern Recognition (CVPR)*, pages 18867–18877, 2023. 2

[59] Kanchana Ranasinghe, Muzammal Naseer, Salman Hameed Khan, Fahad Shahbaz Khan, and Michael S. Ryoo. Self-supervised video transformer. *2022 IEEE/CVF Conference on Computer Vision and Pattern Recognition (CVPR)*, pages 2864–2874, 2021. 2

[60] Hanoona Rasheed, Muhammad Uzair Khattak, Muhammad Maaz, Salman Khan, and Fahad Shahbaz Khan. Fine-tuned clip models are efficient video learners. In *Proceedings of the IEEE/CVF Conference on Computer Vision and Pattern Recognition*, pages 6545–6554, 2023. 8

[61] Mark Sandler, Andrew Howard, Menglong Zhu, Andrey Zhmoginov, and Liang-Chieh Chen. Mobilenetv2: Inverted residuals and linear bottlenecks. In *Proceedings of the IEEE Conference on Computer Vision and Pattern Recognition (CVPR)*, 2018. 2

[62] N. Sayed, Biagio Brattoli, and Björn Ommer. Cross and learn: Cross-modal self-supervision. In *German Conference on Pattern Recognition (GCPR) (Oral)*, Stuttgart, Germany, 2018. 2

[63] Madeline Chantry Schiappa, Naman Biyani, Shruti Vyas, Hamid Palangi, Vibhav Vineet, and Yogesh Singh Rawat. Large-scale robustness analysis of video action recognition models. *ArXiv*, abs/2207.01398, 2022. 5

[64] Madeline C Schiappa, Yogesh S Rawat, and Mubarak Shah. Self-supervised learning for videos: A survey. *ACM Computing Surveys*, 2022. 2

[65] Feifei Shao, Long Chen, Jian Shao, Wei Ji, Shaoning Xiao, Lu Ye, Yueting Zhuang, and Jun Xiao. Deep learning for weakly-supervised object detection and object localization: A survey. *ArXiv*, abs/2105.12694, 2021. 1

[66] Ayush Singh, Aayush J Rana, Akash Kumar, Shruti Vyas, and Yogesh Singh Rawat. Semi-supervised active learning for video action detection. *Proceedings of the AAAI Conference on Artificial Intelligence*, 38 (5):4891–4899, 2024. 2

[67] K. Soomro, A. Zamir, and M. Shah. Ucf101: A dataset of 101 human actions classes from videos in the wild. *ArXiv*, abs/1212.0402, 2012. 3, 2

[68] Nitish Srivastava, Elman Mansimov, and Ruslan Salakhudinov. Unsupervised learning of video representations using lstms. In *Proceedings of the 32nd*

International Conference on Machine Learning, pages 843–852, Lille, France, 2015. PMLR. 1

[69] Xinyu Sun, Peihao Chen, Liangwei Chen, Changhao Li, Thomas H Li, Mingkui Tan, and Chuang Gan. Masked motion encoding for self-supervised video representation learning. In *The IEEE/CVF Conference on Computer Vision and Pattern Recognition (CVPR)*, 2023. 7

[70] Hao Tan, Jie Lei, Thomas Wolf, and Mohit Bansal. Vimpac: Video pre-training via masked token prediction and contrastive learning. *ArXiv*, abs/2106.11250, 2021. 7, 8

[71] Li Tao, Xueting Wang, and Toshihiko Yamasaki. Self-supervised video representation learning using inter-intra contrastive framework. *arXiv preprint arXiv:2008.02531*, 2020. 2

[72] Fida Mohammad Thoker, Hazel Doughty, Piyush Bagad, and Cees G. M. Snoek. How severe is benchmark-sensitivity in video self-supervised learning? In *ECCV*, 2022. 1

[73] Zhan Tong, Yibing Song, Jue Wang, and Limin Wang. Videomae: Masked autoencoders are data-efficient learners for self-supervised video pre-training. *ArXiv*, abs/2203.12602, 2022. 1, 7, 8

[74] Du Tran, Lubomir Bourdev, Rob Fergus, Lorenzo Torresani, and Manohar Paluri. Learning spatiotemporal features with 3d convolutional networks. In *Proceedings of the 2015 IEEE International Conference on Computer Vision (ICCV)*, page 4489–4497, USA, 2015. IEEE Computer Society. 2

[75] D. Tran, H. Wang, L. Torresani, J. Ray, Y. LeCun, and M. Paluri. A closer look at spatiotemporal convolutions for action recognition. In *2018 IEEE/CVF Conference on Computer Vision and Pattern Recognition*, pages 6450–6459, 2018. 3, 1, 2

[76] Aäron van den Oord, Yazhe Li, and Oriol Vinyals. Representation learning with contrastive predictive coding. *ArXiv*, abs/1807.03748, 2018. 1

[77] Carl Vondrick, Hamed Pirsiavash, and Antonio Torralba. Generating videos with scene dynamics. In *Advances in Neural Information Processing Systems*. Curran Associates, Inc., 2016. 1

[78] Jinpeng Wang, Yiqi Lin, Andy Jinhua Ma, and Pong Chi Yuen. Self-supervised temporal discriminative learning for video representation learning. *ArXiv*, abs/2008.02129, 2020. 1, 2, 3

[79] Jiangliu Wang, Jianbo Jiao, Linchao Bao, Shengfeng He, Wei Liu, and Yunhui Liu. Self-supervised video representation learning by uncovering spatio-temporal statistics. *IEEE Transactions on Pattern Analysis and Machine Intelligence*, 44:3791–3806, 2022. 7, 8

[80] Rui Wang, Dongdong Chen, Zuxuan Wu, Yinpeng Chen, Xiyang Dai, Mengchen Liu, Lu Yuan, and Yu-

Gang Jiang. Masked video distillation: Rethinking masked feature modeling for self-supervised video representation learning. In *CVPR*, 2023. 7

[81] X. Wang, K. He, and A. Gupta. Transitive invariance for self-supervised visual representation learning. In *2017 IEEE International Conference on Computer Vision (ICCV)*, pages 1338–1347, 2017. 2

[82] Yi Wang, Yinan He, Yizhuo Li, Kunchang Li, Jiashuo Yu, Xin Ma, Xinyuan Chen, Yaohui Wang, Ping Luo, Ziwei Liu, Yali Wang, Limin Wang, and Yu Qiao. Internvid: A large-scale video-text dataset for multimodal understanding and generation. *arXiv preprint arXiv:2307.06942*, 2023. 8

[83] Jiangliu Watng, Jianbo Jiao, and Yunhui Liu. Self-supervised video representation learning by pace prediction. In *European Conference on Computer Vision*, 2020. 1, 2, 7, 8

[84] Garrett Wilson and Diane Joyce Cook. A survey of unsupervised deep domain adaptation. *ACM Transactions on Intelligent Systems and Technology (TIST)*, 11: 1 – 46, 2020. 1

[85] Dejing Xu, Jun Xiao, Zhou Zhao, Jian Shao, Di Xie, and Yueting Zhuang. Self-supervised spatiotemporal learning via video clip order prediction. In *Proceedings of the IEEE/CVF Conference on Computer Vision and Pattern Recognition (CVPR)*, 2019. 1, 2, 3

[86] Ceyuan Yang, Yinghao Xu, Bo Dai, and Bolei Zhou. Video representation learning with visual tempo consistency. In *arXiv preprint arXiv:2006.15489*, 2020. 2

[87] Xiangli Yang, Zixing Song, Irwin King, and Zenglin Xu. A survey on deep semi-supervised learning. *ArXiv*, abs/2103.00550, 2021. 1

[88] Yuan Yao, Chang Liu, Dezhao Luo, Yu Zhou, and Qixiang Ye. Video playback rate perception for self-supervised spatio-temporal representation learning. *2020 IEEE/CVF Conference on Computer Vision and Pattern Recognition (CVPR)*, pages 6547–6556, 2020. 1, 2, 3

[89] Xiangyu Zhang, Xinyu Zhou, Mengxiao Lin, and Jian Sun. Shufflenet: An extremely efficient convolutional neural network for mobile devices. In *Proceedings of the IEEE Conference on Computer Vision and Pattern Recognition (CVPR)*, 2018. 3, 2

[90] Bin Zhu, Bin Lin, Munan Ning, Yang Yan, Jiaxi Cui, Wang HongFa, Yatian Pang, Wenhao Jiang, Junwu Zhang, Zongwei Li, Cai Wan Zhang, Zhifeng Li, Wei Liu, and Li Yuan. Languagebind: Extending video-language pretraining to n-modality by language-based semantic alignment, 2023. 8

A Large-Scale Analysis on Contextual Self-Supervised Video Representation Learning

Supplementary Material

Here, we explain things in details about pretext task, architecture setup, provide some more results and include more visual analysis. We also include tables which we were not able to include in main paper due to space limitations.

- Section A: describes challenges and future work based on our study.
- Section B: Pretext tasks explanation used in our analysis.
- Section C: Training details about architectures, datasets, and, other hyperparameters.
- Section D: We show additional CKA maps, more results on HMDB51 dataset and more analysis on noise robustness. We added some tables for Knowledge distillation experiments that were promised in the main paper.
- Section E: We extend the main table and compare with previous state-of-the-art results on HMDB51 dataset.

A. Challenges and future work

There are several key challenges in video SSL and we believe 1) long-term video understanding, 2) multi-modal learning, and 3) robust learning are some of the less studied aspects. The novel insights in our study regarding training dataset size, model architectures, and robustness will play a crucial role in guiding future work on these research directions.

B. Pretext Tasks Details

In this section, we go through each pretext task in more detail that are used in our main work for analysis.

B.1. Spatial Transformation

Rotation Net [34] (RotNet)   applies geometrical transformation on the clips. The videos are rotated by various angles and the network predicts the class which it belongs to. Since the clips are rotated, it helps the network to not converge to a trivial solution.

Contrastive Video Representation Learning [56] (CVRL) technique applies temporally coherent strong spatial augmentations to the input video. The contrastive framework brings closer the clips from same video and repels the clip from another video. With no labels attached, the network learns to cluster the videos of same class but with different visual content.

B.2. Temporal Transformation

Video Clip Order Prediction [85] (VCOP)   learns the representation by predicting the permutation order. The network is fed N clips from a video and then it predicts the order from N! possible permutations.

Temporal Discriminative Learning [78] (TDL)   In contrast to CVRL, TDL works on temporal triplets. It looks into the temporal dimension of a video and targets them as unique instances. The anchor and positive belongs to same temporal interval and has a high degree of resemblance in visual content compared to the negative.

B.3. Spatio-Temporal Transformation

Playback Rate Prediction [88] (PRP)   has two branch, generative and discriminative. Discriminative focuses on the classifying the clip's sampling rate, whereas, generative reconstructs the missing frame due to dilated sampling. Thus, the first one concentrates on temporal aspect and second one on spatial aspect.

Relative Speed Perception Network [10] (RSPNet)   applies contrastive loss in both spatial and temporal domain. Clips are samples from a same video to analyze the relative speed between them. A triplet loss pulls the clips with same speed together and pushes clips with different speed apart in the embedding space. To learn spatial features, InfoNCE loss [76] is applied. Clip from same video are positives whereas clips from different videos are negatives.

Video MAE [73] (V-MAE)   applies a spatio-temporal tube masking to the input video. The pretext task is to reconstruct those missing tubes. Mean-squared error loss is applied between the masked tokens and the reconstructed tokens.

C. Implementation Details

C.1. Architecture Details

Preliminary research has shown that 3D networks [27, 75] have outperformed 2D CNN variants on video recognition tasks. We looked into three types of capacity - small, medium and big on the basis of number of trainable parameters. The architecture details of all networks are mentioned in supplementary.

Small capacity networks: are resource efficient, implying they can be trained in larger batches within short span

of time. The network selection is done on the basis of supervised training scores on Kinetics[35] and UCF101[38]. ShuffleNet V1 2.0X [89] utilizes point-wise group convolutions and channel shuffling. SqueezeNet [31] reduces the filter size and input channels to reduce the number of parameters. MobileNet [61] has ResNet like architecture. With its depthwise convolution, there's a reduction in model size and the network can go more deep.

Medium capacity networks: Following the conventional 3D architectures for self-supervised learning approaches C3D, R21D and R3D are used in this study.

Big Capacity networks: Comparing across four transformer architectures, ViViT [5] Timesformer [8], VideoSwin [47] and MViT [18], we selected VideoSwin, because it outperforms others on Kinetics 400 dataset.

Based on [38], we probed into the performance comparison of several versions of these architectures. We choose 3D-ShuffleNet V1 2.0X, 3D-SqueezeNet, and 3D-MobileNet V2 1.0X networks based on their performance on Kinetics and UCF-101 dataset

3D-ShuffleNet V1 2.0X [89]: It utilize point-wise group convolutions and channel shuffling and has 3 different stages. Within a stage, the number of output channel remains same. As we proceed to successive stage, the spatiotemporal dimension is reduced by a factor of 2 and the number of channels are increased by a factor of 2. V1 denotes version 1 of ShuffleNet and 2.0X denotes the 2 times number of channels compared to original configuration.

3D-SqueezeNet [31]: It uses different alteration to reduce the number of parameters as compared to the 2D version which employs depthwise convolution. Those three modifications are: 1) Change the shape of filters from 3x3 to 1x1, 2) Input channels to 3x3 filters is reduced, and, 3) to maintain large activation maps high resolution is maintained till deep layers.

3D-MobileNet V2 1.0X [61]: This network employs skip connections like ResNet architecture in contrast to version 1. It helps the model in faster training and to build deeper networks. There are also linear bottlenecks present in the middle of layers. It helps in two ways as we reduce the number of input channels: 1) With depthwise convolution, the model size is reduced, and 2) at inference time, memory usage is low. V2 denotes version 2 of mobilenet and 1.0X uses the original parameter settings.

The architectures of medium capacity networks are described as follows:

C3D [74]: This follows a simple architecture where two dimensional kernels have been extended to three dimensions. This was outlined to capture spatiotemporal features from videos. It has 8 convolutional layers, 5 pooling layers and 2 fully connected layers.

R3D [27]: The 2D CNN version of ResNet architecture is recasted into 3D CNNs. It has skip connections that helps make the gradient flow better as we build more deeper networks.

R(2+1)D [75]: In this architecture, 3D convolution is broken down into 2D and 1D convolution. 2D convolution is in spatial dimension and 1D convolution is along the temporal dimension. There are two benefits of this decomposition: 1) Increase in non-linearity as the number of layers have increased, and, 2) Due to factorization of 3D kernels, the optimization becomes easier.

VideoSwin [47] It is an inflated version of original Swin [46] transformer architecture. The attention is now spatio-temporal compared to previous which is only spatial. 3D tokens are constructed from the input using patch partition and sent to the network. The architecture includes four stages of transformer block and patch merging layers.

C.2. Original and Noise Datasets

We have shown the examples of each dataset used in the paper in Fig. 6.

The test datasets have different number of videos for different levels and types of noises. For Gaussian noise, we manipulated all 3783 samples. For noise level 1, apart from Gaussian, we had roughly 400 samples and all other levels of severity, we have approximately 550 samples. An example of each type of noise is shown in Fig. 7.

C.3. Pretext Tasks Configurations

Here, we briefly describe the configurations used in our training. For VCOP, RotNet and PRP, we just manipulated the type of augmentation from the original work. We applied Random Rotation, Resizing, Random Crop, Color Jittering and Random Horizontal Flipping to the input clip. CVRL has some extra data augmentation compare to the previous ones we mentioned. It includes grayscale and gamma adjustment as well. RSPNet also uses some temporal augmentation. For finetuning the augmentations are Resize and Center Crop for all the approaches.

The k-value for Momentum contrastive network is 16384 for RSPNet, it's 500 for TDL.

C.4. Datasets

Here we discuss datasets in detail. We use Kinetics-400 (K400) [35] and Something-Something V2 [24] for our pre-training. For the downstream task evaluation, we perform our experiments on UCF-101 [67], HMDB-51 [40], and Diving48 [45]. Since, the pretraining and finetuning datasets are different, the performance variation will provide us a better picture about how much meaningful spatiotemporal features are learned by these networks. K400 has approximately 240k videos distributed evenly across 400 classes respectively. The approximate number of videos in finetuning datasets are: 1) UCF101-10k, 2) HMDB51-7k, and,
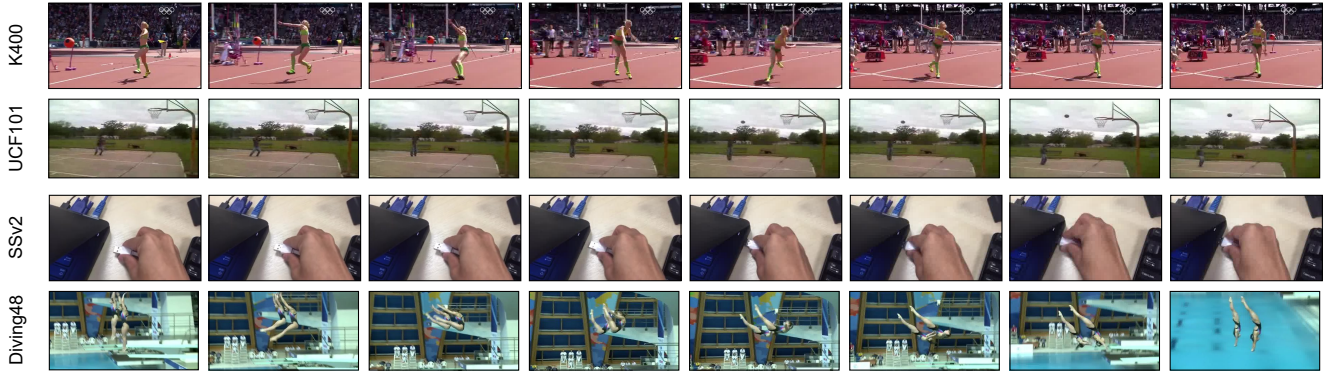
Figure 6. **Example** sample from each dataset.

Figure 7. **Example frame sample for each noise** Gaussian, Impulse, Shot and Speckle from left to right. Sample clips are provided in supplementary.

3)Diving48-16k. The datasets can be categorized into two ways:

Appearance-based: Kinetics, UCF101 and HMDB51 comes under this category [12, 29]. Kinetics videos length are generally 10s centered on human actions. It mainly constitutes singular person action, person-to-person actions and person-object action. For pre-training, we select a random subset of videos and maintain equal distribution from each class. Unless otherwise stated, pre-training is done on K400-50k subset for all experiments.

Temporal-based: In Kinetics, we can estimate the action by looking at a single frame [12, 29]. From Fig. 6, top two rows, we can see the person with a javelin and basketball. This information helps in class prediction. Looking at bottom two rows (SSv2 and Diving48 respectively), we can't describe the activity class until we look into few continuous frames. It shows that temporal aspect plays an important role for these datasets, that's why we categorize them into temporal-based datasets.

UCF-101 [67] : It's an action recognition dataset that spans over 101 classes. There are around 13,300 videos, with 100+ videos per class. The length of videos in this dataset varies from 4 to 10 seconds. It covers five types of categories: human-object interaction, human-human interaction, playing musical instruments, body motion and sports.

HMDB-51 [40] : The number of videos in this dataset is 7000 comprising 51 classes. For each action, at least 70

videos are for training and 30 videos are for testing. The actions are clubbed into five categories: 1) General facial actions, 2) Facial actions with body movements, 3) General body movements, 4) Body movements with object interaction, and, 5) Body movements for human interaction.

D. Additional Results

Here, we will talk about some additional results, to further strengthen the claims made in the main paper.

D.1. Preliminary Experiments

Pretext tasks evaluation Figure 8 depicts the hidden representations of R21D network pretrained on different pretext tasks. Here the 50k subset of K-400 was used for pretraining, and finetuned on UCF-101.

Linear Probing vs Finetuning Firstly, we discuss linear probing (LP) vs finetuning (FT) results for different pretext tasks and different architectures. From Table 9, we can see that FT outperforms LP by a margin of approximately 20% and 40% on ShuffleNet and R21D respectively. Thus, we perform finetuning for all of our analysis.

Network Parameters We have shown the performance across different architectures in Table 10. ShuffleNet and R21D performs the best across small and medium capacity
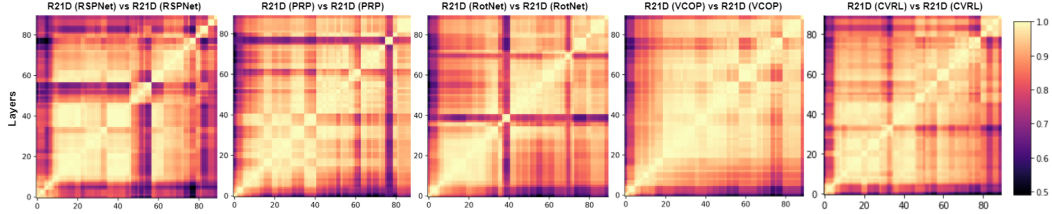
Figure 8. **Pretext tasks CKA maps** for RSPNet, PRP, RotNet, VCOP, CVRL on K-400 50k subset using R21D network (Left to right). R21D pretrained on K400 shows a semi-block structure for VCOP, indicating near-saturation condition of the network on this pretext task. It shows a more prominent grid-based structure on CVRL and RSPNet instead. These observations corroborate the quantitative results, where pretraining on K400 for both CVRL and RSPNet gives better performance.
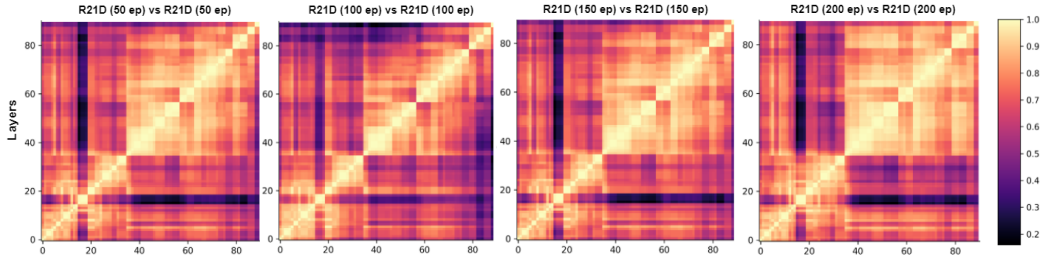
Figure 9. **Training time CKA maps** on 50, 100, 150, 200 epochs of R21D network on RSPNet pretext for K-400 10k subset (Left to right). The block structure is visible from 50 epochs itself, which then darkens and becomes prominent by 200 epochs. With 10k subset, the saturation starts hitting at 100 epochs.

Epochs	Non-contrastive			Contrastive		
	VCOP	Rot	PRP	CVRL	TDL	RSPNet
10k	18.9	15.0	9.2	22.2	9.9	30.2
30k	19.3	11.7	11.5	25.0	10.1	37.3
50k	17.3	12.2	10.2	29.3	9.5	40.2

Table 8. **Evaluation of different pretext tasks** on different subset size on R21D network on HMDB51 dataset.

Network	LP	FT	RotNet	VCOP	PRP
Shuffle	✓		4.3	12.3	2.8
		✓	16.6	40.8	21.9
R21D	✓		2.7	12.2	4.6
		✓	41.2	51.5	46.2

Table 9. **Downstream accuracy** classification on UCF-101 dataset. FT: Finetuning LP: Linear Probing

networks in most of the pretext tasks. Thus, we choose ShuffleNet and R21D for our benchmark analysis.

D.2. Effect of dataset size

In Table 8, we extend results for different pretext tasks on HMDB51 dataset. Similar to UCF101, *the scale in subset size doesn't reciprocate to gain in performance* for all pretext tasks on HMDB51 dataset. From Figures 10 and 11, we see that performance increase for Swin by a good margin, whereas in case of ShuffleNet and R21D it's relatively less beyond 50k subset.

Training time Table 11 shows VideoSwin saturates at 150 epochs on UCF101 whereas CNN architectures saturates earlier (100 epochs) which reflects limitation of model capacity. Figure 9 shows the emergence of block structures for R21D network trained on RSPNet for K400 10k. The saturation point has reached earlier around 100 epochs which supports the hypothesis in main work that CNN architectures mostly saturates around 100 epochs. We see similar pattern even after increasing the dataset size.

D.3. Impact of task complexity

Figures 12 shows for ShuffleNet dark patterns with increase in complexity. R21D shows staggering grids. It supports our hypothesis that *model capacity* plays an important role to learn meaningful features and always increasing the complexity doesn't reciprocate to *better spatio-temporal features*.

D.4. Effect of data distrbituion

Figure 14 illustrates CKA maps for networks pretrained on *different source datasets* - for R21D pretrained on K400-50k

Networks	Parameters	GFLOPs	Rot[†]	VCOP[†]	PRP[†]	RSPNet
ShuffleNet	4.6M	1.1	**42.2**	41.6	**41.1**	68.8
MobileNet	3.1M	1.1	38.0	40.0	37.4	63.1
SqueezeNet	1.9M	1.8	41.3	41.4	39.2	62.9
C3D	27.7M	77.2	**57.7**	54.5	58.1	67.6
R3D	14.4M	39.8	51.1	50.7	52.1	62.1
R(2+1)D	14.4M	42.9	46.9	**56.8**	58.9	**78.0**

Table 10. **Comparison of FLOPs** and trainable parameters for each network on UCF101 dataset. [†] - pretraining on Kinetics 700 [9].

Epochs	Shuffle				R21D				Swin			
	10k	30k	50k	100k	10k	30k	50k	100k	10k	30k	50k	100k
50	59.1	66.3	68.1	68.9	66.8	71.1	75.0	77.2	-	40.4	44.9	52.0
100	60.3	67.6	68.7	69.0	69.5	75.2	76.1	80.0	37.2	44.3	49.6	58.5
150	61.8	66.7	69.4	69.7	69.5	76.6	76.5	78.8	37.9	46.2	50.7	61.3
200	61.5	68.2	68.5	69.9	69.6	76.6	77.4	78.3	36.8	46.3	52.5	61.5

Table 11. RSPNet with different subset size on ShuffleNet/R21D/VideoSwin on UCF101 dataset.
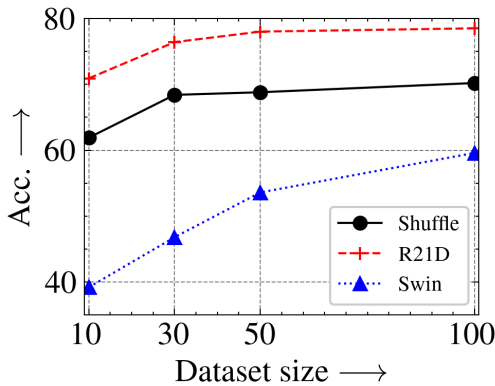
Figure 10. **Multiple architectures and data subsets on UCF101.** Pretext task is RSPNet. (x-axis: subset size, y-axis: Top-1 Accuracy) Here, 10 means 10k dataset subset, 30 means 30k and so on.
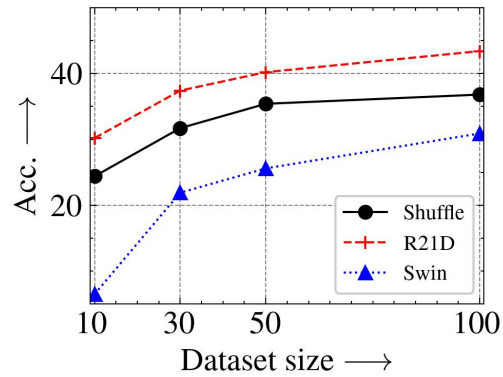
Figure 11. **Multiple architectures and data subsets on HMDB51.** Pretext task is RSPNet. (x-axis: subset size, y-axis: Top-1 Accuracy) Here, 10 means 10k dataset subset, 30 means 30k and so on.

D.5. Robustness of SSL tasks

Table 12 shows performance of each pretext on each type of noise for severity level 1. Fig. 13 shows a relative decrease in performance for three different severity level on UCF101 dataset. *Non-contrastive* tasks are more robust than *contrastive* on average even at different severity levels.

D.6. Feature Analysis

We employ knowledge distillation to evaluate how complementary information from different datasets can be used to train a student model that could take advantage of this in terms of performance gain and training time reduction. Here we show the numbers quantitatively. Table 13 shows smaller architecture leans complementary information whereas bigger architecture depends on pretext task. Table 14 shows that

	Non-contrastive			Contrastive		
	RotNet	VCOP	PRP	CVRL	TDL	RSP
No Noise	41.2	51.5	46.2	61.2	31.7	78.0
Gaussian	40.9	47.0	14.6	12.7	28.0	16.7
Impulse	38.1	30.5	5.4	3.5	18.8	8.5
Shot	33.4	45.1	20.9	26.4	21.5	45.1
Speckle	34.7	43.9	14.4	13.1	24.7	27.0

Table 12. Analysis of all pretext tasks with noise severity level 1 on R21D network on UCF101 dataset.

on VCOP and CVRL respectively. The stark difference in semi-block structure of *spatial (VCOP)* vs grid-like structure of *spatio-temporal (CVRL)* shows spatio-temporal outperforms spatial pretext task.

Figure 12. **Complexity CKA maps** PRP ShuffleNet (Left) and R21D (Right) network increasing complexity from 2 to 4 (Left to right). ShuffleNet has lower performance than R21D, and it shows darkest patterns when complexity is increased from 3 to 4. For both of these complexities, R21D shows staggering grids.
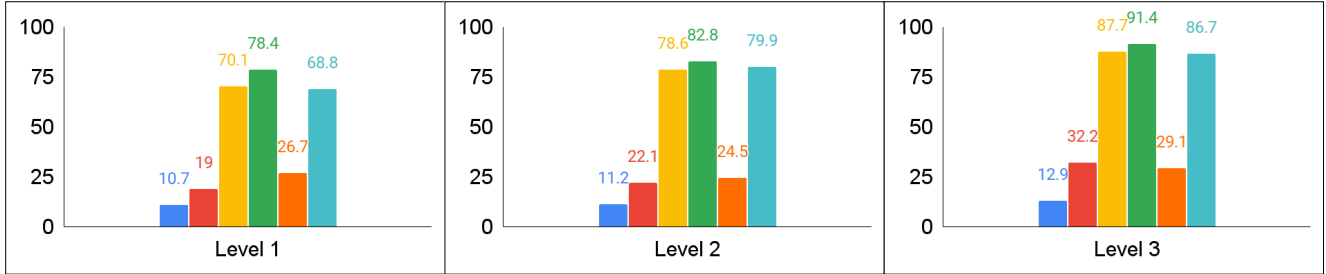
Figure 13. **Relative decrease in performance** at three different severity levels in increasing order from left to right. The pretext tasks is depicted by following colors - RotNet, VCOP, PRP, CVRL, TDL, RSPNet.
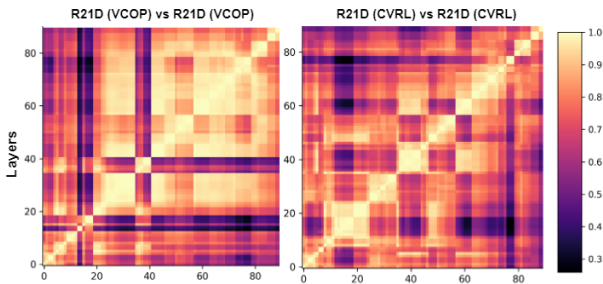
Figure 14. **Out-of-distribution CKA maps:** on VCOP and CVRL for R21D Network (Left to right). The semi-block structure of VCOP contrasts sharply with the grid-like structure of CVRL.

for each pretext task, we learn *complimentary information* from two *different source* datasets. Thus, student always outperforms the teachers. Table 15 shows that distilling knowledge from a *spatial* and a *temporal* task outperforms the standalone *spatio-temporal* task in both *contrastive* and *non-contrastive* case.

D.7. Clip retrieval

In Table 16, we show clip retrieval across different architectures on HMDB51 and UCF101 dataset. Amongst small capacity networks, ShuffleNet outperforms others and in medium-capacity R21D outperforms.

TC↓	RotNet	VCOP	PRP
T1	20.1/48.3	41.6/**56.8**	24.2/38.9
T2	20.2/**58.3**	41.8/54.8	18.1/44.4
T3	16.6/41.2	40.6/55.6	21.9/46.2
S	**75.0**/56.6	**75.4**/43.5	**76.1/61.0**

Table 13. **Complexity variation** with at three levels as teachers (T1, T2, T3) for all three pretext tasks. TC: Task complexity. Results are shown on UCF101 with ShuffleNet/R21D as backbones.

	K400 (T1)	SSV2(T2)	Student
RotNet	36.2	42.5	59.8
VCOP	50.4	59.7	67.6
CVRL	56.9	34.7	66.6
RSPNet	76.4	69.5	80.2

Table 14. **Out-of-Distribution** settings on UCF101 dataset using R21D network with teachers as different *source* datasets.

	S (T1)	T(T2)	Student
Non-Contrastive	RotNet	VCOP	61.1
Contrastive	CVRL	TDL	70.3

Table 15. **Knowledge distillation across different pretext tasks.** Teachers: ShuffleNet; Student: ShuffleNet.

Network	Top@1	Top@5
Squeeze	15.9/38.5	37.6/56.5
Mobile	16.2/37.4	36.5/55.6
Shuffle	19.3/43.1	42.0/62.1
C3D	19.9/43.2	43.4/61.6
R3D	19.3/40.4	42.5/60.2
R21D	18.2/42.7	40.1/62.8

Table 16. Top K Clip Retrieval on HMDB51/UCF101 across different architectures for RSPNet.

E. Main Table

In this section, we firstly expand the Table 6 (main paper) including results on HMDB51 dataset (Table 17). Knowledge distilled network discussed in the main paper still shows competitive performance on HMDB51. Going in depth, the works outperforming us are AVTS[39], GDT [54] in multimodal and VIMPAC [70], VideoMAE [73], TCLR [13] and CVRL [56] in single modality. AVTS and GDT uses two modalities, have more number of frames and AVTS also uses a bigger spatial size. Coming to Generative-based, both VIMPAC and VideoMAE uses a bigger backbone architecture. CVRL uses a longer temporal sequence and bigger frame resolution compared to ours and TCLR utilize 64 effective frames. Thus, the performance on HMDB51 is still competitive.

Approach	Venue	NxW/H	Backbone	Pre-training	UCF101	HMDB51
Generative						
VIMPAC [70]	-	10x256	ViT-L	HTM	92.7	65.9
VideoMAE [73]	NeurIPS'22	16x224	ViT-B	K400	91.3	62.6
VideoMAE * [73]	NeurIPS'22	16x112	R21D-18	K400	76.2	45.4
Context						
PacePred [83]	ECCV'20	16x112	R21D-18	K400	77.1	36.6
TempTrans [32]	ECCV'20	16x112	R3D-18	K400	79.3	49.8
STS [79]	TPAMI-21	16x112	R21D-18	K400	77.8	40.5
VideoMoCo [53]	CVPR'21	16x112	R21D-18	K400	78.7	49.2
RSPNet [10]	AAAI'21	16x112	R21D-18	K400	81.1	44.6
TaCo [6]	-	16x224	R21D-18	K400	81.8	46.0
TCLR[13]	CVIU'22	16x112	R21D-18	K400	88.2	60.0
CVRL[†] [56]	CVPR'21	32x224	R21D-18	K400	92.9	67.9
TransRank [17]	CVPR'22	16x112	R21D-18	K200	87.8	60.1
Multi-Modal						
AVTS [39]	NeurIPS'18	25x224	I3D	K400	83.7	53.0
GDT [54]	-	32x112	R21D	IG65M	95.2	72.8
XDC [4]	NeurIPS'20	32x224	R21D	K400	84.2	47.1
Ours *	-	16x112	R21D-18	K400-30k	97.3	51.5

Table 17. **Comparison with previous approaches** pre-trained on K400. Ours (* best performing) is RSPNet pretrained on 30k subset of K400. [†] modified backbone.